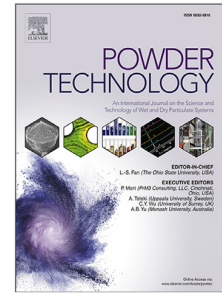


Journal Pre-proof

Modelling segregation phenomena in large industrial silos: A cellular automaton approach

Susantha Dissanayake, Hamid Salehi, Stefan Zigan, Tong Deng,
Michael Bradley



PII: S0032-5910(25)00393-6

DOI: <https://doi.org/10.1016/j.powtec.2025.120998>

Reference: PTEC 120998

To appear in: *Powder Technology*

Received date: 10 February 2025

Revised date: 23 March 2025

Accepted date: 30 March 2025

Please cite this article as: S. Dissanayake, H. Salehi, S. Zigan et al., Modelling segregation phenomena in large industrial silos: A cellular automaton approach, *Powder Technology* (2025), doi: <https://doi.org/10.1016/j.powtec.2025.120998>.

This is a PDF file of an article that has undergone enhancements after acceptance, such as the addition of a cover page and metadata, and formatting for readability, but it is not yet the definitive version of record. This version will undergo additional copyediting, typesetting and review before it is published in its final form, but we are providing this version to give early visibility of the article. Please note that, during the production process, errors may be discovered which could affect the content, and all legal disclaimers that apply to the journal pertain.

© 2025 Published by Elsevier B.V.

Highlights

Modelling Segregation Phenomena in Large Industrial Silos: A Cellular Automaton Approach

Susantha Dissanayake, Hamid Salehi, Stefan Zigan, Tong Deng, Michael Bradley

- Segregation is a prevalent issue in wood pellet handling.
- A Cellular Automaton model was developed to simulate segregation within silos.
- Model predictions were validated against data from laboratory and industrial silos.
- The model demonstrated strong correlation with experimental observations.

Modelling Segregation Phenomena in Large Industrial Silos: A Cellular Automaton Approach

Susantha Dissanayake^a, Hamid Salehi^a, Stefan Zigan^a, Tong Deng^b, Michael Bradley^b

^a*School of Engineering, Faculty of Engineering & Science, University of Greenwich, Central Avenue, Chatham Maritime, ME4 4TB, United Kingdom.*

^b*The Wolfson Centre for Bulk Solid Handling Technology, University of Greenwich, Central Avenue, Chatham Maritime, ME4 4TB, United Kingdom.*

Abstract

Segregation presents a significant challenge in the handling of bulk materials across various industries, including the handling of wood pellets. Wood pellets, which degrade over time, develop a wide particle size distribution, leading to increased segregation during handling. This can result in fines and dust spikes in silo discharge streams, negatively affecting operational efficiency and safety. Accurate prediction of segregation during silo filling and discharging is critical for ensuring safe handling and efficient operations.

To address these challenges, this study develops and validates a Cellular Automata (CA) model to simulate segregation in wood pellet silos. The CA approach provides computational efficiency while capturing the essential physics of particle behaviour. The model was initially calibrated through laboratory experiments and subsequently validated against data from a 2D glass-walled silo. Following successful validation, a 3D CA model was developed and tested against industrial-scale wood pellet silos. The model demonstrated an accurate prediction of segregation patterns and fines content in discharge streams, offering a valuable tool for optimising silo operations and mitigating associated risks.

Keywords: Segregation/ Cellular Automata/ Bulk Materials /Fines Spikes

1. Introduction

Power generation industries are increasingly shifting towards renewable source of energies instead of fossil fuels. In the second quarter of 2024, renewable energy sources accounted for 46.4% of the total electricity generated in the UK [1]. Biomass is a common form of renewable solid fuel used in power generation [2]. It includes firewood, crops, agricultural and forestry residues, and waste [3]. These types of fuels are carbon neutral, meaning biomass emits negligible greenhouse gases over its life cycle. As such, it presents a good alternative for reaching global energy and environmental goals [4, 5] Many coal-fired power stations have been converted to biomass powered power plants in recent years [2, 6], with wood pellets being

Email address: s.dissanayake@greenwich.ac.uk (Susantha Dissanayake)

a typical type of biomass used in these facilities. Wood pellets offer several advantages as an energy source. They are easily stored and transported, and their free-flowing nature simplifies discharge from storage units (where no excessively high fines content). Additionally, wood pellets boast high energy density and efficient pneumatic conveying capabilities. Compared to other fuels, they produce relatively low emissions [7].

Handling and processing wood pellets pose significant challenges, primarily due to particle degradation, which leads to fines and dust formation. This degradation results in a wide “particle size distribution” (PSD) and the phenomenon of segregation when wood pellets are loaded into silos. [8, 9]. Segregation can occur for two main reasons: (i) Differences in particle physical properties: This includes factors such as particle diameter, length, shape, and weight and (ii) Differences in particle dynamics: This includes factors such as the velocity of the carrier air in a pneumatic conveying system, the free-fall height of the particles when filling silos, and the vibration of the silos [10].

Due to the segregation effect, silo discharging can often evidence large variations in fines content over time compared to the input composition of the bulk wood pellets. This creates several issues, such as the occurrence of “saltation” (formation of dunes) during the process of pneumatic conveying [11]. Additionally, there is a potential for the mixture of dust particles with air to escape from the processes, thereby increasing the risk of fires and dust explosions [12, 13] as well as posing health and environmental hazards [14, 15, 16, 17]. Furthermore, the variations in feed streams into the furnaces can result in inefficient burning [18]. Subsequently, the presence of unburned carbon poses challenges in terms of disposal and results in the inefficient utilisation of valuable fuel resources [19]. Consequently, there is an increase in the operational costs associated with cleaning and maintenance.

Predicting fines content in pellet streams is essential to mitigating associated challenges. While existing mathematical modelling offers a potential solution for predicting silo segregation. However, the complexity of mechanistic models, often involving differential and partial differential equations, or higher order derivatives renders them computationally demanding [20, 21, 22, 23]. While computational fluid dynamics, discrete element modelling and other numerical methods are increasingly capable on high-performance computing systems [23, 24], industrial-scale silos on the order of tens of thousands of tonnes of materials often require prohibitively large computational resources, motivating more macroscopic modelling alternatives [25, 26, 27].

To overcome these limitations, this study explores the use of Cellular Automata (CA) modelling to simulate segregation in wood pellet silos. The CA approach, which neglects flow characteristics and focuses on particle kinematics [28, 29], offers a computationally efficient alternative to traditional mechanistic models. Although widely applied in fields such as computer science and biology, CA modelling has had limited applications in bulk material handling [28, 30]. Tejchman [31] simulated flow pattern in silos, while Castro et al. [32] conducted a study to analyse fine migration using cellular automata. The ability of the CA model to simulate complex systems without relying on intricate mathematical formulations makes it a promising tool for large-scale simulations, including segregation predictions [28]. This research aims to develop and validate two-dimensional (2D) CA models for simulating

segregation during silo filling and discharging, using laboratory experiments for calibration. Following successful validation, the model will be extended to three dimensions (3D) and tested against industrial-scale wood pellet silos. By providing accurate predictions of segregation patterns, this study seeks to offer a robust tool for optimising silo operations and enhancing the efficiency of wood pellet handling systems.

2. Method of the CA Modelling

Segregation has several different mechanisms, each with its unique characteristics [33]. The significant primary segregation mechanism that dominates particle heap formation must be clearly recognised before segregation modelling. When silos are filled from the top, particulate materials form a heap, as shown in Figure 1. This figure illustrates half of a particle heap.

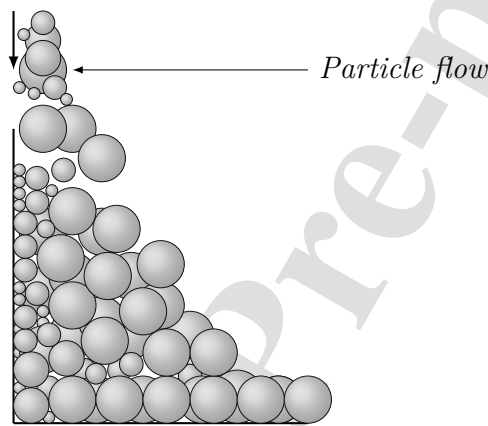


Figure 1: Sieve/Percolation segregation

Coarse particles are placed on the heap, pack loosely while generating much bigger voids. Particles collide on the apex of the heap tend to slide down the sloping particle bed. During this sliding fines and dust permeate through voids created by coarse particles as shown in the Figure 1. As a result of this segregation mechanism, a higher level of fines is arrested closer to the centre of the heap, whereas larger particles are loosely packed and accumulated at the periphery of the heap [33, 34]. This segregation mechanism is known as “sieve/percolation segregation,” and it is equally dominant in silo filling and discharging.

After identifying the primary segregation mechanism, a rule set was developed for the CA models to mimic sieve/percolation segregation behaviours. These rules were implemented on a grid with a finite number of cells. This study focused on examining the composition of particulate materials within a cell, particularly the differential transfer of coarse and fines particles between cells.

The contents of each cell were determined by considering the values of neighbouring cells from the previous time step. Neighbouring cells were defined as those in close proximity to a given cell, following definitions from previous studies [35, 36].

However, adapting CA modelling to bulk solids handling requires careful consideration of the

neighbourhood structure. In conventional CA models, all potential neighbouring cells are considered when calculating a value of a cell in the next time step. In contrast, in bulk solids flow within a heap, these influences are more limited and directional. This is because bulk material movement during heaping and discharge is driven solely by gravity, occurring either vertically or diagonally downward at the angle of repose. Pellets and particles cannot move upward or horizontally. Consequently, the direct use of previously established neighbourhood configurations, such as the von Neumann and Moore neighbourhoods [35, 36], are unsuitable for modelling bulk solids handling.

Thus, the authors established a neighbourhood arrangement for bulk solids modelling. A similar neighbourhood arrangement was used by Castro et al. [32], and a comparable cell migration rule was applied by Kozicki et al. [29]. Figure 2a and Figure 2b shows the revised neighbourhood structure for 2D and 3D CA modelling respectively.

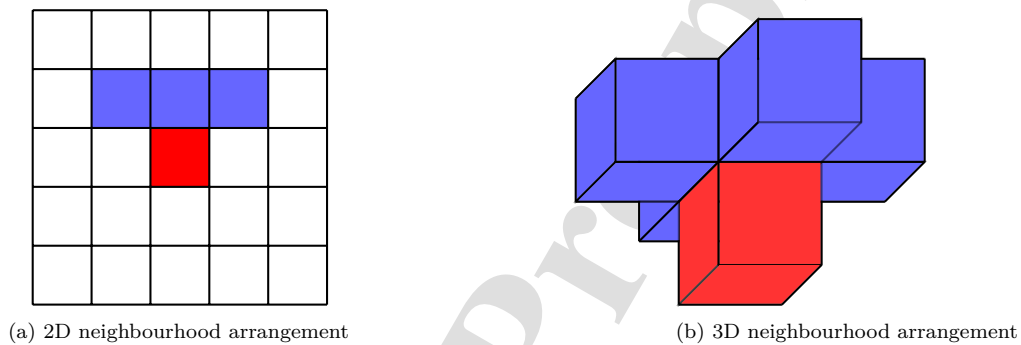


Figure 2: Modified neighbourhood arrangement in the CA modelling.

As shown in Figure 2, only the blue cells affect the properties of the red cell. This means that the cells directly above the red cell, along with one cell to the right and left in the upper (blue) layer, can transport materials into the red cell in the 2D arrangement (Figure 2a). In other words, the top layer of cells around the selected cell constitutes the important neighbourhood in bulk material handling. In the 3D models, the number of neighbours could be considered either five (Figure 2b), or possibly nine if the “corner” cells in the top layer are included.

The model rules, derived from empirical observations of particle movement, were formulated using arithmetic calculations to assess the impact of neighbouring entities. A numbering system (from 0 to 10) was introduced to represent the fines quantity; particle size distribution (PSD) in each cell. Cells with no particles were labelled as “0”, cells filled with just coarse material (clean pellets) were labelled as “1”, and cells filled with particles and filled all spaces with fines (saturated fines) were labelled as “10”. Cells could have intermediate numbers, such as “5”, which indicates that it had filled with coarse materials yet had a “4” degrees of fines.

Through calibration, these integer levels can be mapped onto the measured percentage of fines, enabling the accurate determination of real-world fines content in each cell. The set of rules for silo filling and discharging were following the same principle.

2.1. The 2D CA Model for Silo Filling

In this CA modelling, the set of rules was divided into two parts: (i) Movement of cell bulk contents and (ii) Transfer of fines across cells.

A flat-bottom silo was modelled as a 2D grid of cells with a designated inlet and outlet. During filling, cells were introduced at the top (cell “A” shown in Figure 3) and moved downward to occupy empty spaces as illustrated in Figure 3. Each cell represented a homogeneous mixture of particles with assigned fines content.

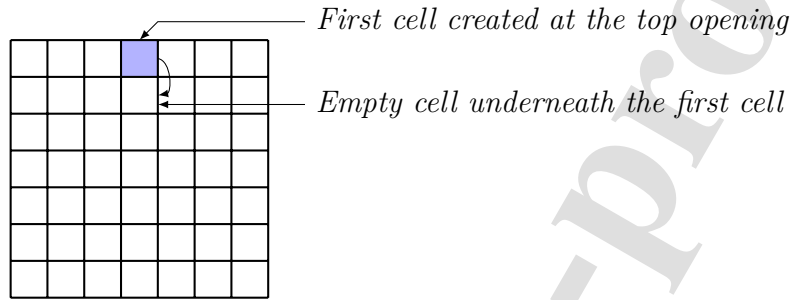


Figure 3: Cell flow in the simulation domain

These motions will continue until the cell “A” reaches the bottom of the grid (Figure 4a).

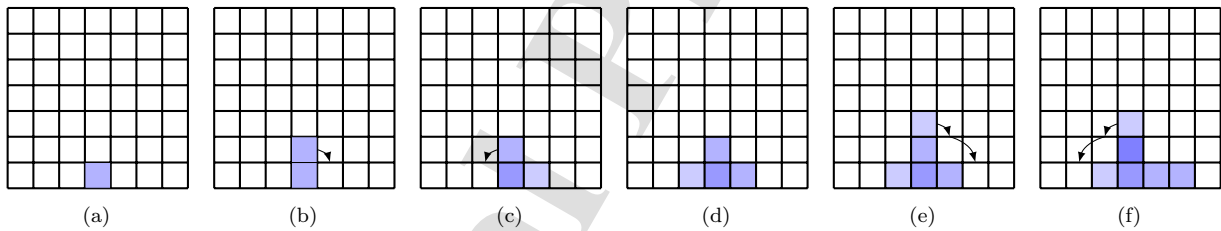


Figure 4: Cell flow in simulation domain

To simulate particle packing, cells were allowed to move diagonally downward when possible, forming a triangular heap structure as illustrated in Figure 4 b,c,d,e and f. The direction of diagonal movement could be random or user-defined. According to the set of rules, particles arrange themselves into a triangular heap structure. The shape of the heap expands as additional cells are introduced at the top, with their diagonal movement playing a defining role.

Subsequent to establishing cell movement rules, a set of rules governing fines transfer between cells was developed. Fines content within a cell remained constant during vertical movement. However, diagonal movement facilitated fines transfer.

The fines transfer mechanism developed in this CA model simplifies the complex percolation phenomena occurring in granular materials. Specifically, the model assumes that fines can move into lower-level cells unless these cells are saturated (i.e., fines number = 10). If the cell

beneath is not saturated, fines are transferred until either the cell beneath becomes saturated or the source cell is depleted. Cells without fines (i.e., fines number = 1) do not contribute to fines transfer. As a result, this simplified approach, combined with the cell movement rules, produces a triangular heap with varying fines content, reflecting segregation patterns during filling.

This assumption does not explicitly capture pore-scale effects such as void networks [37], bridging, or group-trapping [38, 39]. According to Duran [40], free percolation occurs only when the fine-to-coarse size ratio is below 0.15. The predictive accuracy of the CA model depends on both this size ratio and the proportion of fines present. When fines exceed a critical threshold (typically 15% of the coarse particle size), they are more likely to become trapped, limiting their mobility. Additionally, a broad size distribution may introduce effects such as cohesive clustering or air entrainment, which are not explicitly addressed by the current form of the CA model.

Industrial wood pellets, typically cylindrical in shape with a length of 6 mm are large enough to facilitate percolation [41]. Unlike spherical or irregular granular materials, cylindrical pellets exhibit anisotropic flow properties due to their tendency to align along preferred orientations [42]. In the development of the CA model, cell movement is governed by bulk segregation trends rather than individual particle orientations. Although anisotropic effects are not explicitly captured at the particle level, the calibration process ensures that model predictions align with observed segregation patterns, incorporating the macroscopic impact of pellet shape.

In Appendix 1 show the filling algorithm.

2.2. The 2D CA Model for Silo Discharging

The silo discharge model consisted of two main components: cell movement and inter-cellular fines transfer, similar to the filling model. Discharge initiated with the opening of the silo outlet. Cells were removed from the bottom outlet, creating an empty space that can propagate upward as cells repositioned to fill the voids, a process known as upward void propagation. Fines content remained unchanged during these vertical movements. This upward movement of empty spaces formed a channel above the outlet. Figure 5 illustrates the channel above the outlet after several discharge cycles.

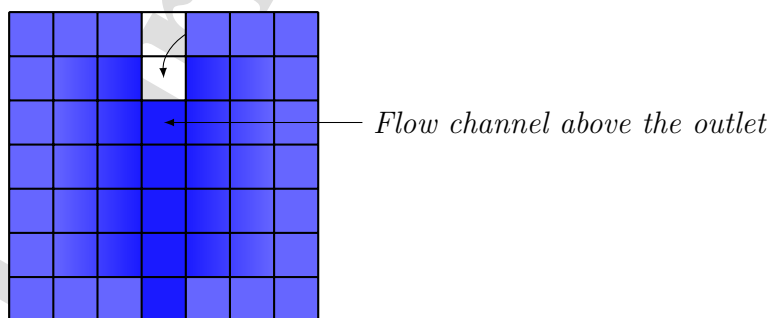


Figure 5: Flow channel created during material discharge

When a channel reached the silo top, the top right cell filled the void, and the left cell occupied the vacated space. This process initiated a funnel-shaped flow pattern that continued until discharge ceased as shown in Figure 6. To replicate realistic flow behaviour, this study employed rectangular cells with an adjustable aspect ratio, allowing user to calibrate the angle of repose to match experimental measurements.

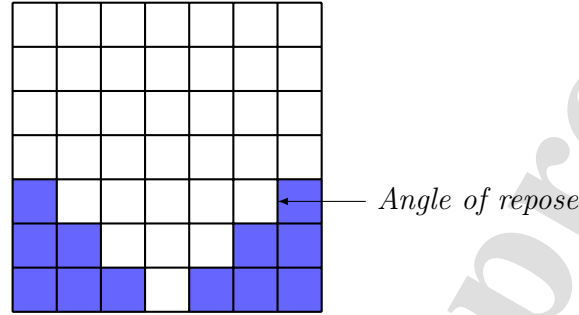


Figure 6: Flow stop at the angle of repose

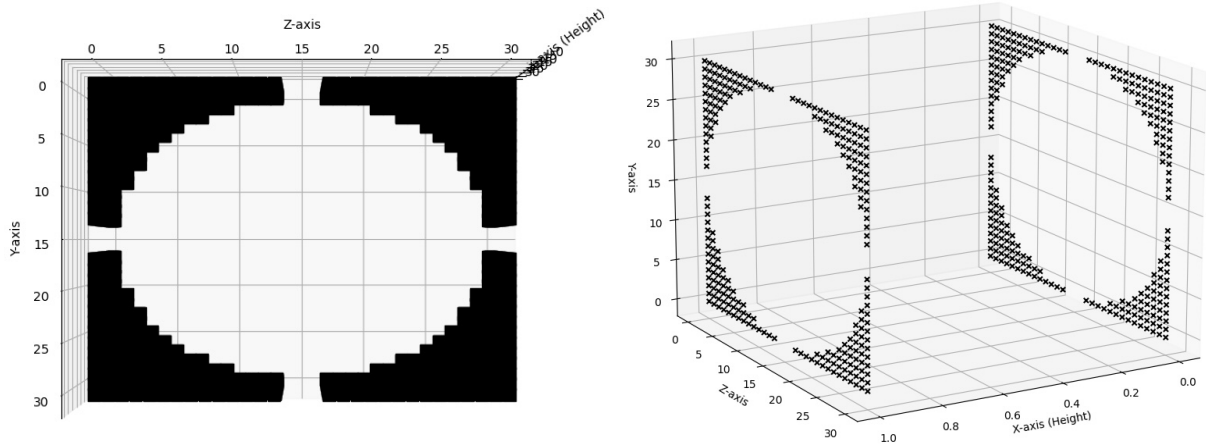
Fines transfer during discharge followed the same rules established for the filling process: fines were transferred to unsaturated cells during diagonal movements. To facilitate simulations, algorithms were developed for both filling and discharging processes (see Algorithm 2 for detailed pseudocode).

2.3. Method of Converting the 2D CA Models into 3D Models

The 2D CA models were extended to 3D models using a modified four-cell neighbourhood arrangement (Figure 2b). A cuboidal grid was initially created to represent 3D simulation domain, however to accurately represent cylindrical silo geometries, fixed cells were introduced to confine the simulation domain. This approach allowed for the creation of various silo shapes within the cuboidal framework. A cylindrical shape, for instance, was generated by inscribing a circle within the x and y plane of the cuboid, defined by Equation 1.

$$y^2 + z^2 - r^2 = 0 \quad (1)$$

Values of y and z in the equation is y and z coordinates. r is the radius of the circular plan view, i.e. radius of the silo. Subfigure (a) in Figure 7 shows the identified cells covered by the equation in 1. Black cells represent fixed cells which correspond to the cylinder wall. The numbers on the x-axis align with each other in the plan view.



(a) Identify cells in the border in cuboid matrix (Plan view)

(b) Identify cells in the border across the height in cuboid matrix

Figure 7: Combined subfigures showing cell identification in the cuboid matrix.

Cells within the circular area were assigned a specific number, while those outside were designated as inactive ‘border cells’ with a unique identifier. This pattern was replicated throughout the grid’s height. Figure 7 subfigure (b) illustrates the layered structure of the 3D cuboidal grid. For clarity, only the top and bottom layers are shown. This method can be adapted to create other shapes as required [43].

2.4. Convergence test to explore minimum domain size needed for 3D model

To optimise computational efficiency, a convergence study was conducted to determine the minimum required number of cells. Cuboidal grids with varying volumes, while maintaining the aspect ratio of a real 30,000-tonne wood pellet silo, were simulated. The silo shape was approximated as a cylinder inscribed within a 3D cuboid matrix. By analysing the normalised discharge streams from these simulations, an optimal cell count was established. Table 1 presents the grid dimensions used in this analysis, where the volume progression refers to the ratio of domain volumes used to test convergence.

Table 1: Round shaped domain sizes used for convergence test.

Width	Depth	Height	Cells available for filling	Volume progression
11	11	25	2225	1.0
13	13	30	3630	1.6
16	16	37	7659	3.4
17	17	39	8307	3.7
18	18	41	10455	4.7
19	19	43	11223	5.0
20	20	46	14674	6.6
21	21	48	15600	7.0
22	22	50	18950	8.5
23	23	53	20405	9.2
27	27	62	33790	15.2

Results for the convergence testing are discussed in section 3.4.2.

After that, the 2D CA models were converted into 3D CA models. The algorithms of the 3D models were shown in the appendix (Algorithm 3 and 4).

2.5. Computing techniques

To assess the CA models, computer based simulations were conducted. A 2D grid, representing a cross-sectional slice of a silo, was implemented in the model. Initially, a low-resolution grid was employed to facilitate visualisation of cellular details. Users could adjust height and width parameters to achieve desired resolution levels.

The 3D grid accurately represented the entire cylindrical silo. Initially, inflow cells were assigned a consistent fines content. Python, along with the PyCharm IDE¹, was used to solve the models. Graphical representations were generated using imshow from the Matplotlib library². While square cells are depicted here, rectangular cells can be implemented to reflect the material's angle of repose. Cells exiting the domain were tracked, stored in arrays, and visualised using Python's plotting functionalities.

Simulations were conducted on a standard Apple Mac mini computer equipped with a 3.2 GHz 6-core processor highlighting the model's ability to run on readily available hardware. Following simulations, the CA models were validated and calibrated through laboratory experiments. Subsequently, the 3D models were tested against data from industrial silos.

2.6. Calibration of the segregation model

A Bench Scale Segregation Tester (BSST) (Figure 8) was employed to calibrate the 2D CA filling models. Prior research by Abou-Chakra [44] demonstrated the BSST's ability to accurately simulate segregation patterns across various scales, from kilograms to thousands of tonnes. The BSST, with a capacity of 8-10 kg, comprised a feeding hopper, a bed with

¹<https://www.jetbrains.com/pycharm/>

²<https://matplotlib.org/stable/gallery/index.html>

adjustable tilt, five bed separators, and a stainless-steel hopper. The length of the BSST bed is 1.2 m, and the width is 21 cm. The bed, surfaced with sandpaper to provide roughness on pellet sliding. BSST could be inclined to match the wood pellet angle of repose. Pellets rolled down the inclined bed, mimicking the behaviour of particles within a wood pellet heap.

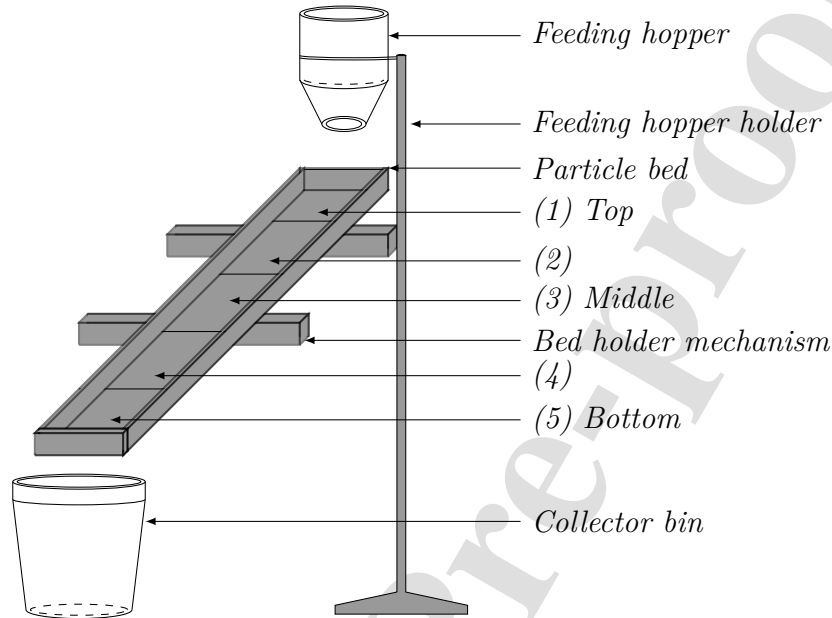


Figure 8: Bench Scale Segregation Tester (BSST)

Wood pellet samples, typically 30-40 mm in length and 6-8 mm in diameter at manufacture, were collected and subsequently subjected to sieve analysis to determine their particle size distribution. Particles smaller than 500 μm were classified as dust, while those between 500 μm and 3.15 mm round (*mmR*) were considered fines. As the models simulate cumulative fines and dust, all particles passing through the 3.15 mm round (*mmR*) sieve were used for calibration.

The angle of repose for wood pellets was determined through a standard pour test [45]. The BSST bed angle was subsequently adjusted to match this value. The feeding hopper was positioned at a height of 15 cm above the bed to ensure a free flow of particles while minimising bouncing effects. A well-mixed batch of wood pellets was carefully loaded into the hopper to prevent segregation in hopper filling. Gradual hopper opening allowed pellets to flow onto the bed, where they distributed evenly due to the matched angle of repose. A 10 cm thick pellet layer formed on the bed. Finally, the contents of each BSST bed section were collected and sieved to quantify fines concentration. Those values were used to compute a calibration curve, presented in Section 3.2. It was utilised to establish a quantitative relationship between the model's fines content scale (1-10) and the experimentally measured fines percentage range. This curve enabled the translation of model predictions into real-world fines content values. A linear calibration approach was employed in this study and the calibration factor was iteratively adjusted to optimise the agreement between model

predictions and experimental data from the BSST. Through this process, the model was successfully calibrated to accurately replicate experimental outcomes. The calibration curve was then used to align discharge model predictions with actual fines percentages.

2.7. Validation against 2D model in laboratory

A glass-panelled 2D silo (Figure 9) was specifically designed and constructed for the calibration and validation of the 2D CA model. Dimensions of 57 *cm* in height, 53 *cm* in width, and 6 *cm* in depth were chosen. This silo facilitated visual observation of the discharge process. The 6 *cm* depth was deliberately chosen to minimise particle movement along the z-axis and prevent jamming. The silo had a capacity of 8-10 *kg* of wood pellets and featured interchangeable discharge openings ranging from 4 *cm* to 8 *cm*. To reduce particle bouncing during the filling process, a feeding tube was strategically positioned at the silo's center. Wood pellets were introduced into the silo through a funnel located at the opposite end of the tube, ensuring a controlled and smooth filling process.

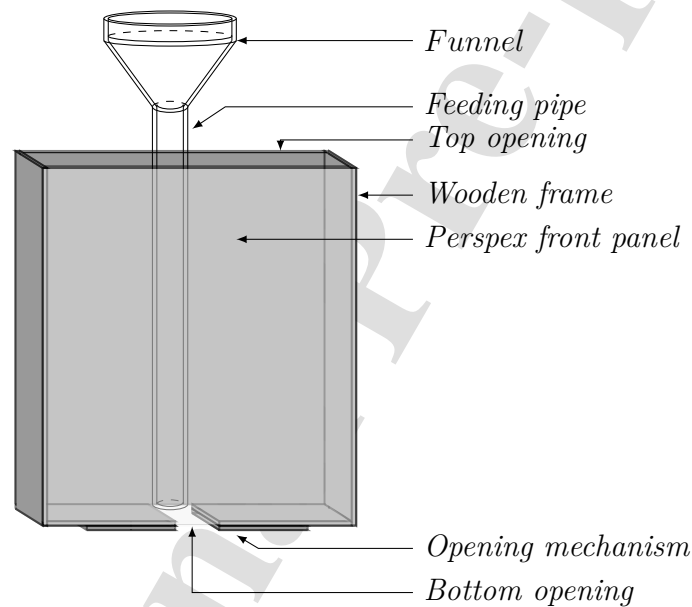


Figure 9: 2D silo design

A wood pellet batch was sieved through a 3.15 *mmR* sieve to separate fines from clean pellets. Subsequently, 880 *g* of clean pellets and 120 *g* of fines were mixed and carefully loaded into the feeding tube to avoid segregation. Once filled, the tube was slowly lifted and refilled as needed. After filling, the silo outlet was opened, and the discharged pellets were collected and sieved to determine fines content. This experiment determined the fines levels and their distribution pattern, providing data for the validation of the discharge model. The model-predicted discharge outcomes were then calibrated using the calibration curve discussed earlier and compared with the experimental results.

2.8. Method of the 3D Model Analysis Against Industrial Silos

Two concrete silos, each with a diameter of 36.5 m, height of 56.5 m, and a capacity of approximately 30,000 tonnes, were selected at Immingham Port, England, for validation of the 3D model. The silos feature a flat bottom design and were loaded centrally from the top to maintain symmetrical distribution, thereby minimising uneven stress on the side walls. Silo 2 and Silo 3 were designated based on their location within the silo array shown in Figure 10.



Figure 10: Silos at Immingham port³

Silo 2 initially contained 8900 tonnes of pellets with unknown fines content, while Silo 3 began empty at the drained angle of repose. The ship discharge line was equipped with an automatic sampling unit that collected a 1-tonne sample for every 2,340 tonnes of material unloaded. These samples were analysed in-house to determine fines content, providing detailed inflow fines data at consistent 2,340-tonne intervals during the ship unloading and silo filling process. Silo 2 reached a final fill level of 14,625 tonnes, while Silo 3 attained 15,568 tonnes. Similar automatic sampling was employed for discharge stream analysis. Inflow pellet fines content fluctuated due to ship cargo segregation. A linear calibration curve was drawn using the experimental data shown in Table 10 and Table 10 in the Appendix. This calibration curve was applied to align inflow fines percentage with model inputs. Model-predicted discharge data was then compared with experimental measurements for validation purposes.

3. Results and Discussion

This section presents the simulation and model validation exercise for both the 2D and the 3D CA models.

3.1. Results for the 2D CA Filling and Discharging Models Validations

Figure 11 presents simulation results for the 2D CA model. The 20×21 cell grid (total 420 cells) was filled with 310 cells, each initially containing a fines level of “3” (out of a maximum of 10). Dark brown cells indicate higher fines content, while light brown cells

represent fines-free areas (value of 1). The background is shaded in light gray to enhance the clarity of the images.

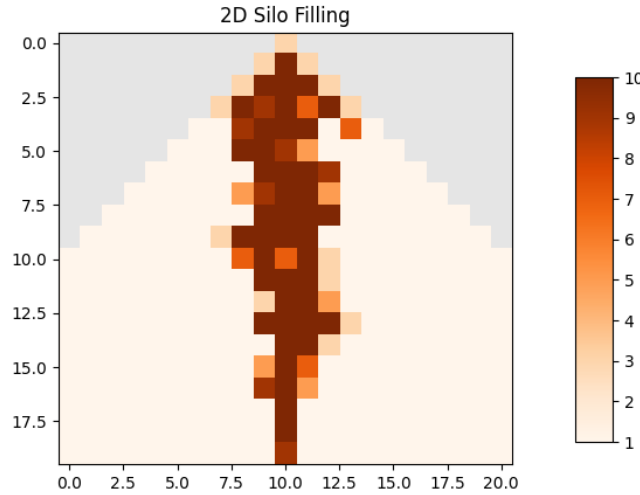


Figure 11: Simulation of filling of 2D silo

Figure 11 illustrates a clear segregation pattern, with fines concentrating at the silo center and diminishing towards the walls. Preliminary simulations demonstrated the computational efficiency of the 2D CA model, significantly outperforming other modelling techniques [24]. A 100×51 cell domain required seven minutes, while a 20×21 domain shown in the Figure 11 took less than three seconds on a standard desktop computer, achieving the study's primary objective of rapid simulation.

3.2. Calibration of the CA model

Figure 12 presents the input material analysis conducted in the Wolfson Centre laboratory, revealing 1.6% dust and 12.5% fines, totalling 14% fines content. A batch of wood pellets was received from Drax Power, and a sample with a high fines content was selected to enhance segregation for observation purpose during the experiment. In this step, the fine-to-coarse size ratio defined by Duran [40] was considered to ensure the free flow of particles.

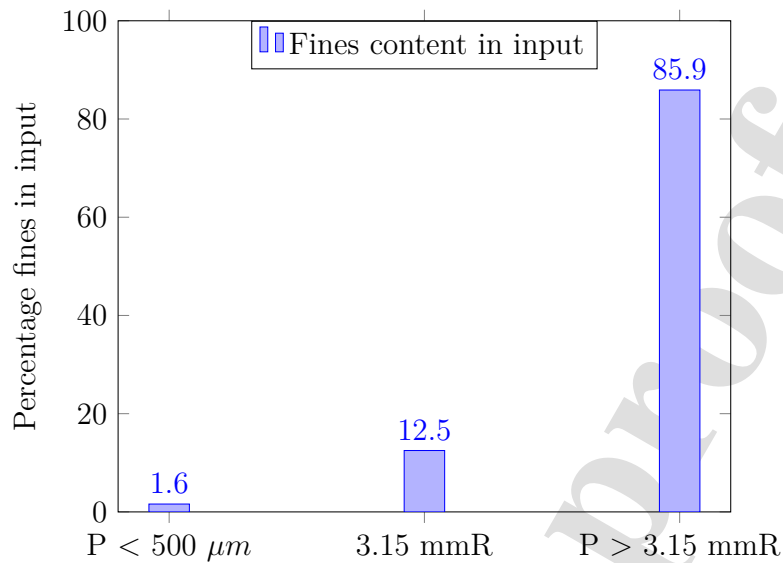


Figure 12: Characterisation of input pellets

The wood pellet angle of repose was measured as approximately 33 degrees. The BSST bed angle was adjusted accordingly, and a test was conducted. Subsequent analysis determined the fines content in different BSST segments, as shown in Figure 13.

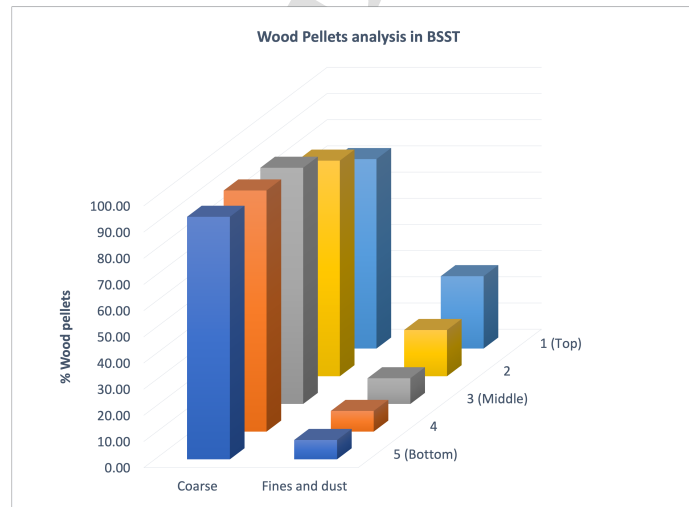


Figure 13: Results of BSST analysis

Figure 13 clearly illustrates a concentration gradient of fines within the BSST, with a significantly higher proportion accumulating at the top. Approximately 27.4% of fines were recovered from the BSST top, while 7.3% were found at the bottom. Negligible fines loss, estimated at around 0.2%, occurred during the experimental process.

Table 2 summarises the extreme fines content values obtained from the BSST analysis. These

data points, representing maximum and minimum fines concentrations, served as the basis for model calibration. In this study,

- Coarse pellets were assigned a value of “1”
- Empty cells were designated as “0”
- The maximum fines content value (27.64%) corresponded to a model predicted outcome of “10”.
- The minimum fines content value (7.38%) was assigned a value of “1”, representing the lower end of the scale.

This numerical representation formed the basis of the calibration curve used in the 2D filling model.

Table 2: Calibration data for 2D filling model

	Fines in BSST	Model predicted outcomes
Maximum fines	27.64	10
Minimum fines	7.38	1
Coarse pellets		0
Empty cell		0

Figure 14 shows the calibration curve drawn using the information given in the Table 2.

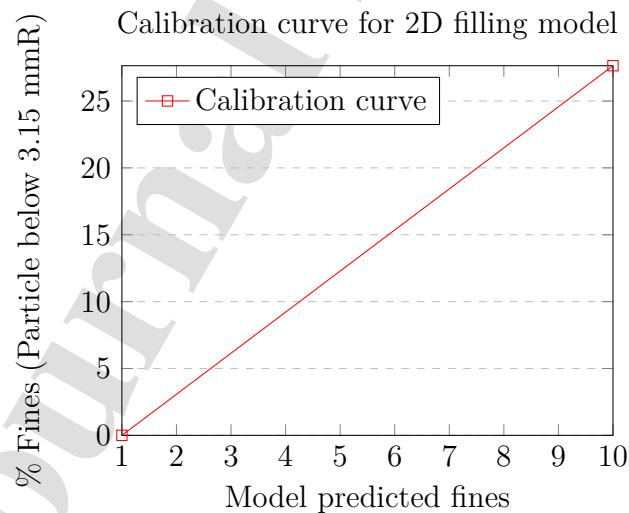


Figure 14: Calibration curve for 2D filling model

The results of the simulation were calibrated using the linear equation derived from the calibration curve (Figure 14). The CA model requires calibration to map its internal

integer scale (1–10) to real-world fines percentages. A linear calibration curve was applied consistently throughout this study.

Table 3 compares the average fines content from four experimental trials with the calibrated model predictions.

Table 3: Calibrated data for 2D filling model

Experimental Fines Content (%)	Original Model Predictions (%)	Calibrated Model Predictions (%)
27.64	9.90	27.33
17.66	7.00	18.43
9.8	4.80	11.67
7.90	3.30	7.06
7.38	1.50	1.54

A plot of the calibrated model-predicted outcomes versus the experimental data is shown in Figure 15. The error bars for the four experiments are also displayed in the figure.

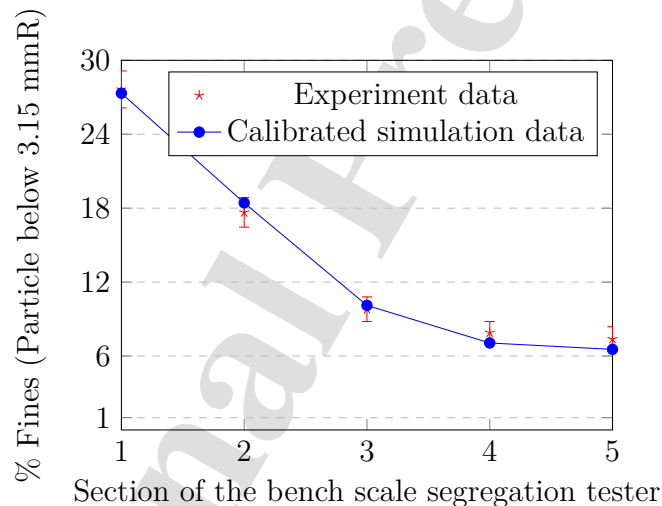


Figure 15: Calibration of simulation data with experimental data

Figure 15 demonstrates a strong correlation between the calibrated model predictions and the experimental data points. The inclusion of error bars provides a clearer representation of variability within the experimental data, reinforcing the reliability of the observed trends. The model assumes unrestricted movement of fine particles between cells based on the fine-to-coarse size ratio threshold suggested by Duran [40], while disregarding the cohesive nature of wood pellets, particularly when the fines content exceeds 0.15 [46]. The slight discrepancy between the experimental fines content and the calibrated model predictions suggests potential resistance to fine particle transport in real-world conditions. Despite this, the overall agreement between model predictions and experimental data, while

accounting for the variability indicated by the error bars is promising given the model's simplicity. Thus, the model remains a valuable tool for predicting fines segregation patterns during wood pellet heap formation.

3.3. Discharge model validation

The 2D CA discharge model was simulated, and the results are visualised in Figure 16. The simulation completed in under three seconds. As illustrated in Figure 16, the model accurately predicts the complete discharge of fines through the outlet, with the remaining material forming a stable angle of repose composed majority of clean pellets.

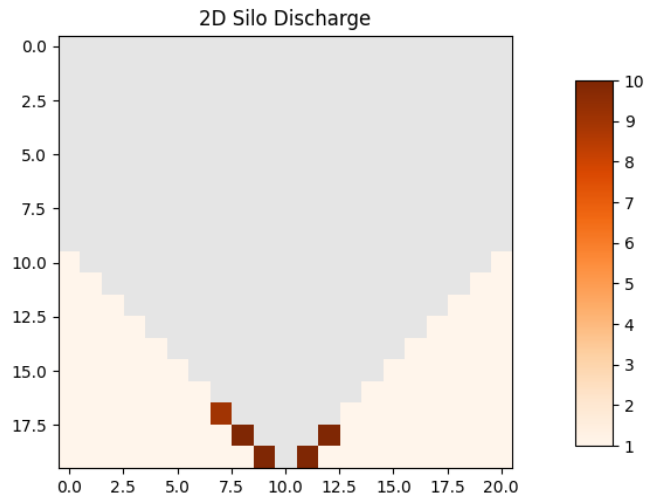


Figure 16: Simulation of discharge of 2D silo

To validate the 2D CA discharge model, a pellet stream was collected from the outlet of a glass-walled 2D silo. During the discharge 11 equal portions of samples were withdrawn from the silo. Each portion was sieved to quantify its fines content, and the model-predicted fines were calibrated accordingly. The test was conducted four times, and the average fines content was calculated for analysis. The errors in the data set are plotted. Table 4 shows the averaged experimental results, model predicted outcomes, and the calibrated model predicted outcomes.

Table 4: Calibrated data for 2D CA discharging model

Sample Number	Experiment Data	Simulation Data
1	11.34	11.50
2	19.18	20.10
3	22.35	22.50
4	24.87	24.13
5	19.46	19.69
6	15.58	15.00
7	12.43	14.38
8	10.00	10.88
9	10.34	10.01
10	12.37	12.88
11	11.85	11.38

The plot of the experimental data versus the calibrated model predicted outcomes had shown in Figure 17.

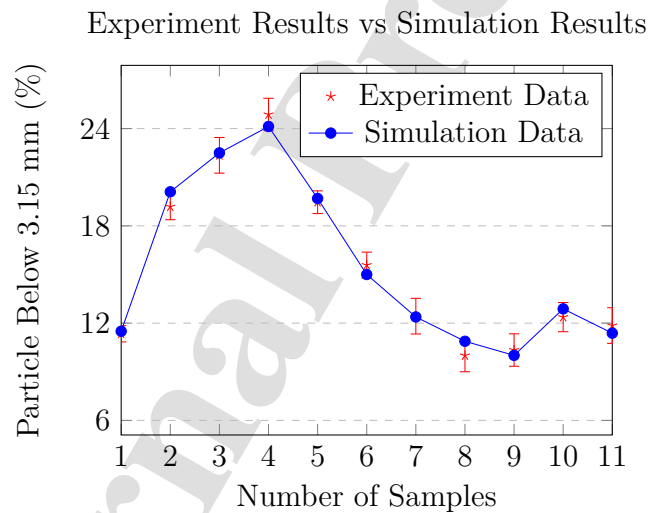


Figure 17: The experimental data versus the calibrated model predicted outcomes

Figure 17 demonstrates the strong predictive capability of the developed models for fines content in the discharge process. While a slight discrepancy between model predictions and experimental data is observed, a t -test was performed to assess its statistical significance. Table 5 presents the calculated values for both experimental and model-predicted data. Table 5 summarises the mean difference and standard deviation between the two datasets. The calculated t -value is 0.0903. Comparing this to the critical t -value of 2.086 (obtained from the t -table for a significance level of 0.05 and 20 degrees of freedom), we conclude that the observed difference is not statistically significant.

Table 5: T-test results

Parameter	Value
Mean (Experiment)	15.43
Mean (Simulation)	15.68
Standard Deviation (Experiment)	5.20
Standard Deviation (Simulation)	5.05
Degrees of Freedom	20
Critical t-value ($\alpha = 0.05$)	2.09
t-Statistic	-0.11

As the calculated t – *value* is smaller than the critical t – *value*, the null hypothesis is accepted. This indicates no statistically significant difference between the experimental and model-predicted outcomes. The high correlation between the calibrated model predictions and experimental data, as evidenced by the t – *value*, is crucial for identifying fines spikes during discharge. By Figure 17, it is possible to predict fluctuations in fines content during the discharge process, facilitating the development of strategies to manage these peaks.

3.4. Progressing Towards 3D Model Validation

Having established the validity and accuracy of the 2D CA model through rigorous laboratory testing, the focus now shifts to validating its three-dimensional counterpart. The following section presents the results of applying the 3D CA model to simulate wood pellet segregation in industrial-scale silos.

3.4.1. Creating cylindrical domain

This section explores the creation of cylindrical shaped domains and the determination of optimal cell numbers for 3D modelling. Figure 18 illustrates the plan view of a cylindrical domain, where black cells represent fixed boundaries, and white spaces indicate active cells for filling and discharging operations.

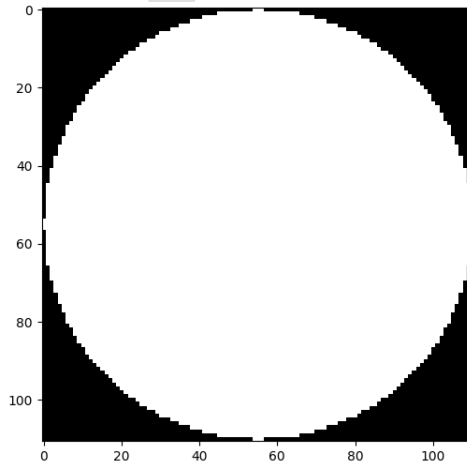


Figure 18: Cross section of a round cylindrical domain0

3.4.2. Optimum domain size/number of cells for 3D CA models

Figure 19 presents the results of a convergence study to determine the optimal number of cells required for accurate simulations. The discharge data arrays have different lengths; therefore, they were normalised for comparison. The x-axis shows the normalised discharge, while the y-axis represents the model-predicted fines contents.

Subfigure 19a in top left side summarises, six domains with varying dimensions from 11×25 to 19×43 . Subfigure 19b, in top right side includes an additional five larger domains size varying from 20×46 to 27×62 . Figure 19c highlights the domains exhibiting convergence.

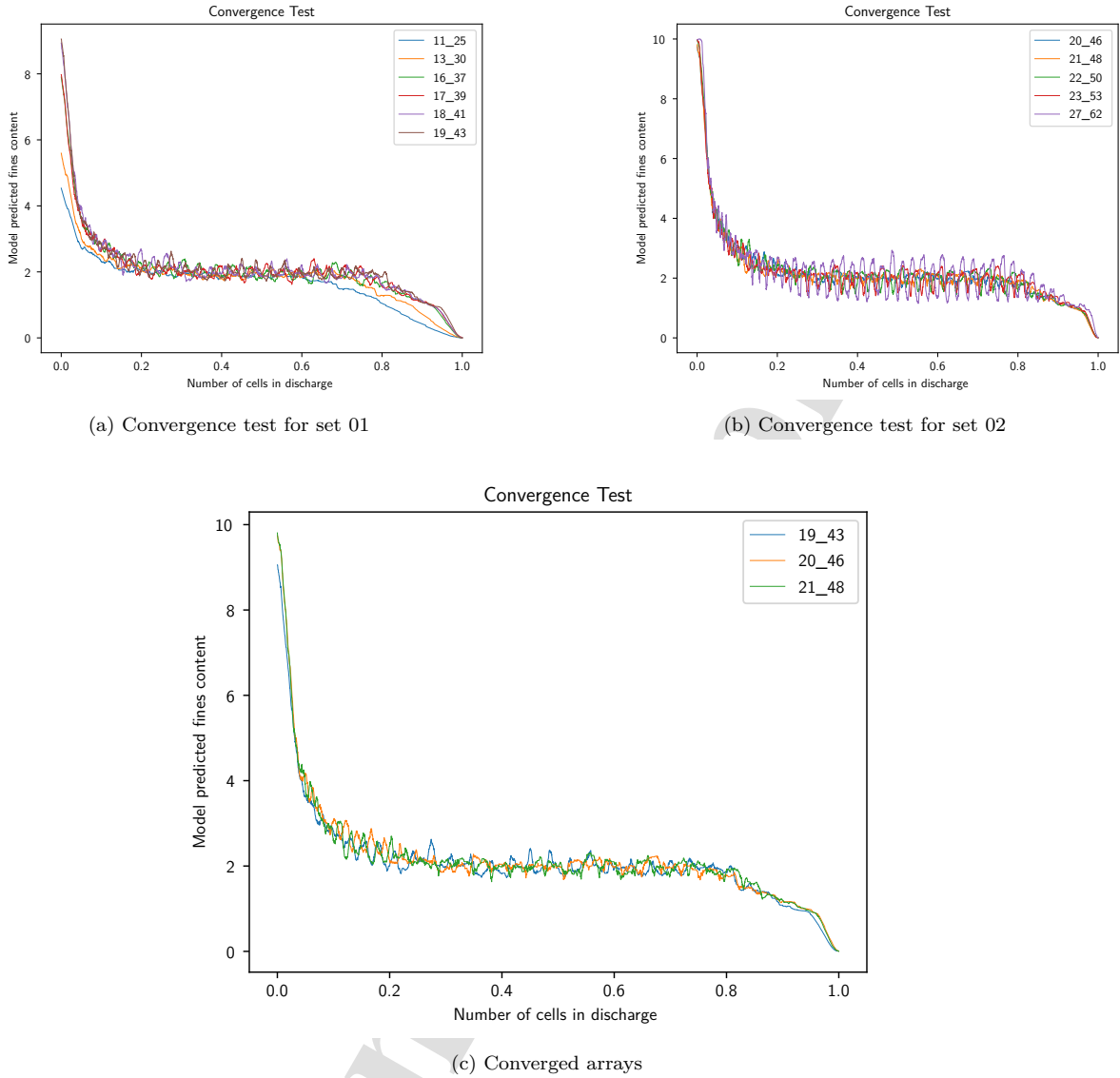


Figure 19: Convergence test for different size domains

Smaller size domains showed in Figure 19 (e.g., 11×25) inconsistent results, indicating insufficient resolution for reliable predictions. However, according to the Figure 19, domains with dimensions of 19×43 , 20×46 , and 21×48 demonstrated convergence, where the predicted fines distributions remained stable despite further increases in domain size. Larger domains generally converged as well, though the largest domain (27×62) exhibited cyclical oscillations, likely due to numerical resonance effects.

To balance computational efficiency and accuracy, we selected a domain size of 21×48 (15,600

cells), which demonstrated convergence and achieved stable predictions. This domain required approximately 3 hours of simulation time, compared to 12 hours for the largest domain (27×62). Averaging the results across convergent domains (19×43 to 27×62) yielded outcomes similar to those of the 21×48 domain, confirming its adequacy for the study.

3.5. Results of the 3D CA Model Validations

The 3D models underwent validation using the same methodology as the 2D CA models. Linear calibration curves were employed to determine the integer values corresponding to the actual weight percentage of inflow fines content. The data used to compute this calibration curve is provided in Table 10 in the Appendix.

Table 6: Experimental and calibrated data for silo 2 filling

Sample point	mid	Actual (wt.%)	Fines	Calibrated inflow fines levels (wt.%)
1170		10.4		10
3510		9.2		9
5850		7.5		7
8190		5.8		6
10530		5.3		6
12870		4.6		5

The “Sample mid point” listed in Table 6 refers to the midpoint of a single subplot, which corresponds to 2340 tonnes.

3.6. Silo 3 filling and emptying

Silo 2 initially contained 8,900 tonnes of pellets with an unknown fines content. To isolate the impact of known material, the model was pre-filled with 8,900 cells, each assigned a fines level of 3 to represent the existing materials. Due to the first-in, last-out nature of flat-bottom silos, the unknown material is discharged at the end of the process. To mitigate this, the user stopped withdrawal before the unknown material is released.

Subsequently, cells with known fines content, delivered from ship were introduced into the silo. The simulation recovered 14,200 cells, matching the actual filling amount. Figure 20 presents simulation results, with dark brown areas indicating fine accumulation and light brown representing coarse particles.

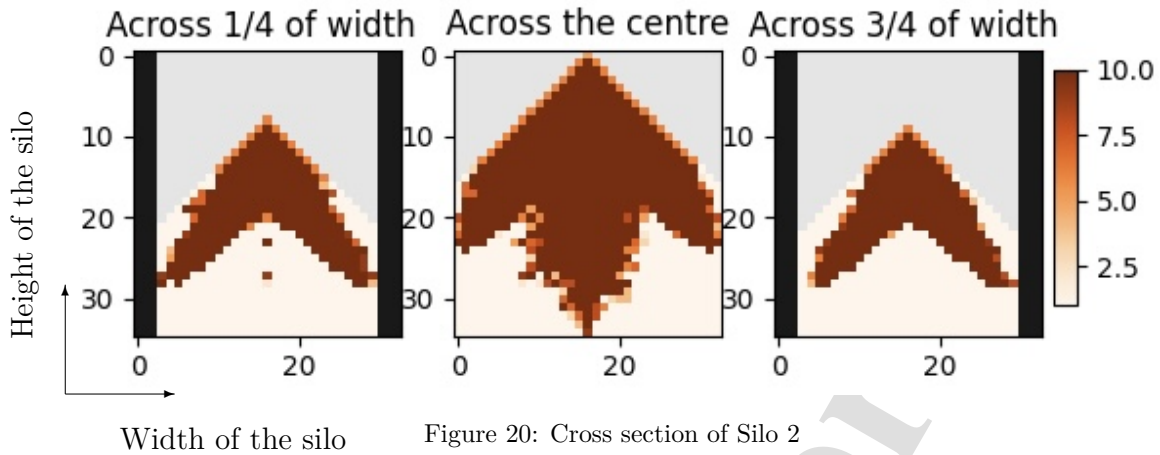


Figure 20: Cross section of Silo 2

Experimental data from Immingham Silo 2 was converted into model-equivalent integer values using the calibration curve and plotted alongside the model predicted outcome. Table 7 summarises the sampling point, actual fines content, and calibrated values. Discharge sampling posed significant logistical challenges due to shifting schedules and changing personnel responsibilities. As a result, sampling was conducted on an opportunistic basis, relying on the engineer's reminders to ensure data collection. The first sample was taken after 1650 tonnes had been withdrawn from the ship.

Table 7: Experimental data for Silo 2 discharge

Sample point	Fines (wt.%)	Calibrated fines level (wt.%)
1650	19.1	10.00
4950	12.8	7.03
9900	13.4	7.31
11550	13.6	7.41

Figure 21 shows the model predicted outcomes as a solid line. The experimental data points are shown as red dots.

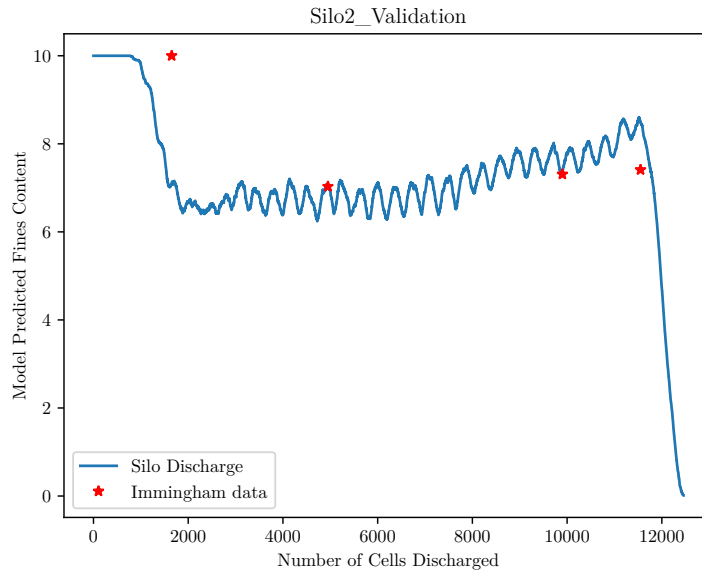


Figure 21: Silo 2 Validation with experiment data.

This predictions followed the measured fines discharge fairly closely, so the model was considered to be validated for this case. In this case, the models produced its outcomes in 3 hours and 45 minutes.

3.7. Silo 3 filling and emptying

The 3D CA model was validated against data from Immingham Silo 3 using the same methodology as for Silo 2. However, the varying fines content in the Silo 3 feedstock provided an opportunity to test the model under different operating conditions. Inflow fines content was analysed and used to construct a calibration curve (Table 11 in Appendix). Model input integers were derived from this calibration curve, as summarised in Table 8.

Table 8: Experimental data for Silo 3 filling

Sample point	Mid	Actual (wt.%)	Fines	Calibrated inflow fines levels (integers)
15210		4.7		4
17550		2.9		3
19890		2.3		3
22230		3.4		3
24570		12.8		10
26910		7.8		6
29250		7.5		6

A total of 15,568 tonnes of wood pellets were loaded into Silo 3. Importantly, the filling process began at the drained angle of repose, necessitating a non-empty initial state for the simulation grid. Model simulations produced predicted outcomes, while experimental data points were converted into model-equivalent integer values using the calibration curve (Table 9).

Table 9: Experimental data for Silo 3 discharge

Sample point	Actual fines	Calibrated data
1650	26	10.00
6600	15.9	6.50
11500	9.5	4.29
13200	8.8	4.05

Model-predicted fines content was plotted against experimental data points in Figure 22. The solid line represents the model's output, while red stars indicate experimental data.

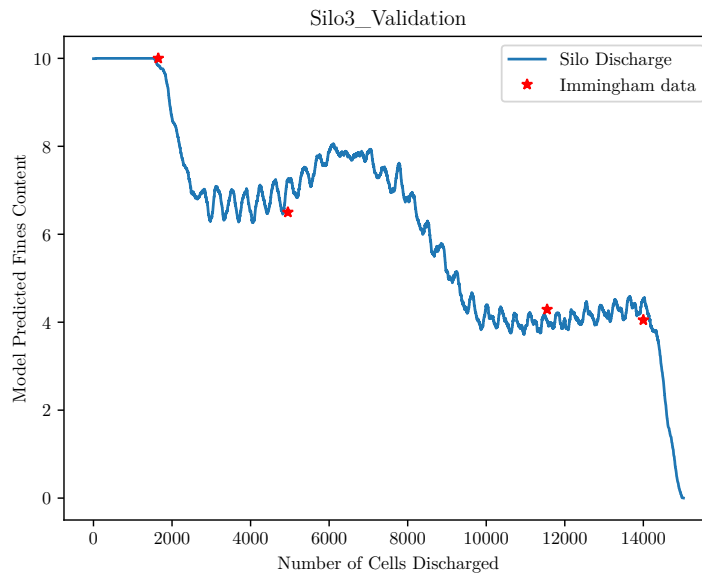


Figure 22: Silo 3 Validation with experiment data

The 3D CA models accurately predicted distinct fines patterns in the discharge from both silos, demonstrating successful validation. Silo 3, which received a higher fines concentration towards the end of filling, exhibited elevated fines levels during the initial discharge phase due to core-flow discharge. Conversely, Silo 2, with early fines enrichment, displayed increased fines content in the latter part of discharge.

Figures 21 and Figure 22 illustrate the model's ability to capture the essential features of fines variation in both silos, despite limited plant data. The clear distinction between the two

patterns strongly supports the use of 3D CA models for predicting segregation in industrial silos.

While this study primarily focuses on wood pellets, the methodology presented in this work is based on general principles of granular flow and cellular automata (CA) modelling. These principles can, in theory, be extended to other types of bulk materials.

However, the specific parameters, such as particle size distribution, density, and cohesion, would need to be considered for each material type, as these factors can significantly influence the movement behaviour. For instance, materials with a higher degree of cohesion or a wider range of particle sizes, such as powders or irregularly shaped materials, may require additional modifications to the movement criteria or calibration process.

These variations may necessitate adjustments to the assumptions made in the current model, such as the representation of pore-scale effects [37, 38] or the handling of bridging and trapping phenomena. As for developing a general method for constructing movement criteria, this remains a challenging yet promising area of research. While it is possible to develop a more generalised framework, it would need to account for the diverse behaviours observed in different bulk materials. Future work could explore how material-specific factors such as particle shape, surface roughness, and moisture content could be incorporated into a more universal set of movement rules. This could potentially allow for a broader application of the CA model across various types of granular materials.

4. Conclusion

This study successfully validated the accuracy of both 2D and 3D cellular automaton (CA) models in simulating silo filling and discharging processes. Through a combination of laboratory experiments and industrial-scale testing, the models demonstrated a strong ability to predict free-surface segregation within silos, with a 95% confidence level agreement between model-predicted and experimental results.

The CA approach's reliance on simple, logical rules and mathematical calculations offers significant adaptability and flexibility, especially when compared to more complex models. The models effectively handle varying fines content without requiring fundamental changes, showcasing their potential for addressing a wide range of bulk material handling challenges beyond silo segregation. Notably, the CA models can handle multiple inlets, outlets, and variable fines content in inflow streams without requiring modifications to the underlying rules.

Furthermore, the CA method's macroscopic perspective allows for larger simulation domains compared to particle-based methods, leading to significantly reduced computational costs. This efficiency, coupled with the model's accuracy, positions CA as a valuable tool for industrial applications.

Although the current models focus on a single primary segregation mechanism and exclude cohesive or collision-driven segregation, their successful validation opens the door for applications in optimising silo design, operations, and safety, particularly in industries such as biomass storage and food processing. The model's capabilities allow for the integration with real-time monitoring systems to enhance operational efficiency and material flow management.

Additionally, incorporating advanced rules to account for multi-mechanism segregation and flow channels could further improve the accuracy and applicability of the CA models. Future work could greatly benefit from integrating multi-field coupling with the CA model, particularly through the combination of CA with Computational Fluid Dynamics (CFD) to model gas-solid interactions. This would help better capture the dynamic behaviour of particles in environments where gas flow influences the movement and segregation of particles. Gas-solid two-phase flow, for example, is known to significantly affect the flow and packing behaviour of powders in industrial silos, which could provide a more accurate representation of particle dynamics in such systems.

CRediT authorship contribution statement

Susantha Dissanayake: Conceptualisation, Methodology, Investigation, Formal analysis, Writing-original draft. **Hamid Salehi:** Formal analysis, Writing-review & editing. **Stefan Zigan:** Supervision, Formal analysis, Writing,-review & editing. **Tong Deng:** Supervision, Formal analysis, Writing,-review & editing. **Michael Bradley:** Funding acquisition, Conceptualisation, Supervision, Writing-review & editing.

Declaration of Competing Interest

The authors declare that they have no known competing financial interests or personal relationships that could have appeared to influence the work reported in this paper.

Acknowledgement

This work was supported by the Net Zero research (formerly Biomass and Fossil Fuel Research Alliances (BF2RA)) in the UK and the Wolfson Centre for Bulk Material Handling Technology.

References

- [1] D. for Business Energy & Industrial Strategy, “National statistics overview: Energy trends: September 2021,” Aug. 8 2024.
- [2] M. Balat and G. Ayar, “Biomass energy in the world, use of biomass and potential trends,” *Energy sources*, vol. 27, no. 10, pp. 931–940, 2005.
- [3] T. Bridgwater, “Biomass for energy,” *Journal of the Science of Food and Agriculture*, vol. 86, no. 12, pp. 1755–1768, 2006.
- [4] B. Mola-Yudego, M. Selkimäki, and J. R. González-Olabarria, “Spatial analysis of the wood pellet production for energy in europe,” *Renewable Energy*, vol. 63, pp. 76–83, 2014.

- [5] L. Nunes, J. C. Matias, and J. P. Catalao, "Wood pellets as a sustainable energy alternative in portugal," *Renewable Energy*, vol. 85, pp. 1011–1016, 2016.
- [6] C. Wang, Y. Chang, L. Zhang, M. Pang, and Y. Hao, "A life-cycle comparison of the energy, environmental and economic impacts of coal versus wood pellets for generating heat in china," *Energy*, vol. 120, pp. 374–384, 2017.
- [7] R. Ireland, "The rise of utility wood pellet energy in the era of climate change," 2022.
- [8] N. Engblom, H. Saxén, R. Zevenhoven, H. Nylander, and G. G. Enstad, "Segregation of powder mixtures at filling and complete discharge of silos," *Powder technology*, vol. 215, pp. 104–116, 2012.
- [9] T. P. Dudziak, K. Jahns, D. Wilk Kołodziejczyk, U. Krupp, A. Polkowska, V. Deodeshmukh, and M. Warmuzek, "Internal oxidation prediction by cellular automata approach in energy materials at high temperatures," *Advanced Engineering Materials*, vol. 21, no. 7, p. 1801142, 2019.
- [10] M. Alizadeh, A. Hassanpour, M. Pasha, M. Ghadiri, and A. Bayly, "The effect of particle shape on predicted segregation in binary powder mixtures," *Powder Technology*, vol. 319, pp. 313–322, 2017.
- [11] E. Rabinovich and H. Kalman, "Boundary saltation and minimum pressure velocities in particle–gas systems," *Powder Technology*, vol. 185, no. 1, pp. 67–79, 2008.
- [12] E. Salzano, "Confined gas and dust explosions," 2014.
- [13] R. K. Eckhoff, *Dust explosions in the process industries: identification, assessment and control of dust hazards*. elsevier, 2003.
- [14] A. C. Rohr, S. L. Campleman, C. M. Long, M. K. Peterson, S. Weatherstone, W. Quick, and A. Lewis, "Potential occupational exposures and health risks associated with biomass-based power generation," *International journal of environmental research and public health*, vol. 12, no. 7, pp. 8542–8605, 2015.
- [15] K. S. Galea, M. Van Tongeren, A. J. Sleuwenhoek, D. While, M. Graham, A. Bolton, H. Kromhout, and J. W. Cherrie, "Trends in wood dust inhalation exposure in the uk, 1985–2005," *Annals of occupational hygiene*, vol. 53, no. 7, pp. 657–667, 2009.
- [16] P. Rekhadevi, M. Mahboob, M. Rahman, and P. Grover, "Genetic damage in wood dust-exposed workers," *Mutagenesis*, vol. 24, no. 1, pp. 59–65, 2008.
- [17] T. Kauppinen, R. Vincent, T. Liukkonen, M. Grzebyk, A. Kauppinen, I. Welling, P. Arezes, N. Black, F. Bochmann, F. Campelo, *et al.*, "Occupational exposure to inhalable wood dust in the member states of the european union," *The Annals of occupational hygiene*, vol. 50, no. 6, pp. 549–561, 2006.

- [18] Z. Sánchez Castro, P. Gauthier-Maradei, and H. Escalante Hernández, “Effect of particle size and humidity on sugarcane bagasse combustion in a fixed bed furnace,” *Revista ION*, vol. 26, no. 2, pp. 73–85, 2013.
- [19] M. Variny and O. Mierka, “Improvement of part load efficiency of a combined cycle power plant provisioning ancillary services,” *Applied Energy*, vol. 86, no. 6, pp. 888–894, 2009.
- [20] H. K. Versteeg and W. Malalasekera, *An introduction to computational fluid dynamics: the finite volume method*. Pearson education, 2007.
- [21] T. J. Barth and J. A. Sethian, “Numerical schemes for the hamilton–jacobi and level set equations on triangulated domains,” *Journal of Computational Physics*, vol. 145, no. 1, pp. 1–40, 1998.
- [22] S. Jiménez and L. Vázquez, “Analysis of four numerical schemes for a nonlinear klein-gordon equation,” *Applied Mathematics and Computation*, vol. 35, no. 1, pp. 61–94, 1990.
- [23] S. Dissanayake, R. Sharma, and B. Lie, “Semi discrete scheme for the solution of flow in river tinnelva,” in *2016 9th EUROSIM Congress on Modelling and Simulation*, pp. 134–139, EUROSIM Electronic Press, 2016.
- [24] S. Dissanayake, R. Sharma, and B. Lie, “Third Order Reconstruction of the KP Scheme for Model of River Tinnelva,” *Modeling, Identification and Control*, vol. 38, no. 1, pp. 33–50, 2017.
- [25] L.-L. Zhao, Y.-W. Li, X.-D. Yang, Y. Jiao, and Q.-F. Hou, “Dem study of size segregation of wet particles under vertical vibration,” *Advanced Powder Technology*, vol. 30, no. 7, pp. 1386–1399, 2019.
- [26] H. Xiao, Y. Fan, K. V. Jacob, P. B. Umbanhowar, M. Kodam, J. F. Koch, and R. M. Lueptow, “Continuum modeling of granular segregation during hopper discharge,” *Chemical Engineering Science*, vol. 193, pp. 188–204, 2019.
- [27] S. He, J. Gan, D. Pinson, and Z. Zhou, “Particle shape-induced radial segregation of binary mixtures in a rotating drum,” *Powder Technology*, vol. 341, pp. 157–166, 2019.
- [28] J. Kozicki and J. Tejchman, “Application of a cellular automaton to simulations of granular flow in silos,” *Granular Matter*, vol. 7, no. 1, pp. 45–54, 2005.
- [29] J. Kozicki and J. Tejchman, “Simulations of flow patterns in silos with a cellular automaton: part 1,” *TASK Quarterly. Scientific Bulletin of Academic Computer Centre in Gdansk*, vol. 9, no. 1, pp. 81–102, 2005.

- [30] C. Picioreanu, M. C. Van Loosdrecht, and J. J. Heijnen, “Mathematical modeling of biofilm structure with a hybrid differential-discrete cellular automaton approach,” *Biotechnology and bioengineering*, vol. 58, no. 1, pp. 101–116, 1998.
- [31] J. Tejchman and J. Tejchman, “Simulations of flow pattern with cellular automaton,” *Confined Granular Flow in Silos: Experimental and Numerical Investigations*, pp. 455–492, 2013.
- [32] M. H. de Castro, J. A. M. da Luz, and F. de Orquiza Milhomem, “Cellular automaton-based simulation of bulk stacking and recovery,” *journal of materials research and technology*, vol. 16, pp. 263–275, 2022.
- [33] J. Carson, “Understanding and eliminating particle segregation problems,” *Bulk Solids Handling*, vol. 6, pp. 139–144, 1986.
- [34] D. Schulze, “Powders and bulk solids,” *Behaviour, Characterization, Storage and Flow*. Springer, vol. 22, 2008.
- [35] L. B. Kier, P. G. Seybold, and C.-K. Cheng, *Modeling chemical systems using cellular automata*. Springer Science & Business Media, 2005.
- [36] L. Maignan and J.-B. Yunes, “Moore and von neumann neighborhood n-dimensional generalized firing squad solutions using fields,” in *2013 First International Symposium on Computing and Networking*, pp. 552–558, IEEE, 2013.
- [37] R. Mirghafari, S. S. Sajjadian, E. Nikooee, G. Habibagahi, and A. Raof, “A pore network modeling approach to bridge void ratio-dependent soil water retention and unsaturated hydraulic conductivity curves,” *Engineering Reports*, vol. 6, no. 12, p. e13012, 2024.
- [38] R. Mirghafari, S. Sajjadian, E. Nikooee, G. Habibagahi, and A. Raof, “A pore network modeling approach to bridge void ratio-dependent soil water retention and unsaturated hydraulic conductivity curves,” *Engineering Reports*, vol. 6, 09 2024.
- [39] A. Kerimov, G. Mavko, T. Mukerji, and M. A. Al Ibrahim, “Mechanical trapping of particles in granular media,” *Phys. Rev. E*, vol. 97, p. 022907, Feb 2018.
- [40] J. Duran, *Sands, powders, and grains: an introduction to the physics of granular materials*. Springer Science & Business Media, 2012.
- [41] A. Nicolas, Á. Garcimartín, and I. Zuriguel, “Trap model for clogging and unclogging in granular hopper flows,” *Physical review letters*, vol. 120, no. 19, p. 198002, 2018.
- [42] T. Börzsönyi, B. Szabó, S. Wegner, K. Harth, J. Török, E. Somfai, T. Bien, and R. Stannarius, “Shear-induced alignment and dynamics of elongated granular particles,” *Phys. Rev. E*, vol. 86, p. 051304, Nov 2012.

- [43] M. F. Guasti, “Analytic geometry of some rectilinear figures,” *Int. J. Math. Educ. Sci. Technol*, vol. 23, no. 6, pp. 895–901, 1992.
- [44] H. Abou-Chakra, U. Tüzün, I. Bridle, M. Leaper, M. Bradley, and A. Reed, “Assessing the potential of a fine powder to segregate using laser diffraction and sieve particle size measuring techniques,” *Advanced Powder Technology*, vol. 14, no. 2, pp. 167–176, 2003.
- [45] M. A. Madrid, J. M. Fuentes, F. Ayuga, and E. Gallego, “Determination of the angle of repose and coefficient of rolling friction for wood pellets,” *Agronomy*, vol. 12, no. 2, p. 424, 2022.
- [46] D. Barletta, R. J. Berry, S. H. Larsson, T. A. Lestander, M. Poletto, and Á. Ramírez-Gómez, “Assessment on bulk solids best practice techniques for flow characterization and storage/handling equipment design for biomass materials of different classes,” *Fuel Processing Technology*, vol. 138, pp. 540–554, 2015.

5. Appendix

Algorithm 1 Pseudo code/Algorithm for 2D filling model

```

max_fines = maximum fines in a cell (Cell number=10)
min_fines = minimum fines in a cell (Cell number =1)

count=0
while count<filling cycles, do
  for each cell in height and width, do
    if cell > 0 and cell underneath =0, then
      cell moves to the empty cell underneath
    end if
    if cell > 0 and the cell underneath > 0 and , cell left =0 or cell right t= 0, then
      selected cell move to the empty cell underneath
    end if
    if cell < max_fines then
      transfer fines from left or right cell:
      fines_transferred = min(fines in left cell, fines in right cell)
      cell += fines_transferred
    end if
    if cell > max_fines then
      transfer excess fines to adjacent cells:
      fines_transferred = cell - max_fines
      cell= max_fines
    else
      no fines transfer
    end if
  end for
  count+=1
end while

```

Algorithm 2 Pseudo code/Algorithm for 2D discharge model

```

max_fines=maximum fines in a cell (Cell number =10)
min_fines=minimum fines in a cell (Cell number =1)

count=0
while count<discharge cycles, do
  for each cell in height and width, do
    if cell = 0 and cell above it  $\neq$  0, then
      cell moves to the empty cell
    end if
    if cell = 0 and the cell above = 0 and , cell left or cell right  $\neq$  0, then
      selected cell move to the empty cell underneath
    end if
    if cell < max_fines then
      transfer fines from left or right cell:
      fines_transferred = min(fines in left cell, fines in right cell)
      cell += fines_transferred
    end if
    if cell > max_fines then
      transfer excess fines to adjacent cells:
      fines_transferred = cell- max_fines
      cell= max_fines
    else
      no fines transfer
    end if
  end for
  count+=1
end while

```

Algorithm 3 Pseudo code/Algorithm for 3D silo filling model

```

max_fines =maximum fines in a cell (cell number =10)
min_fines =minimum fines in a cell (cell number =1)
border= (any number > max_fines)

count=0
while count<Filling cycles, do
  for each cells in height, width, and depth, do
    if any cell > 0 and cell underneath = 0, then
      Cell moves to the empty cell
    end if
    if cell > 0 and the cell underneath > 0 and cell north, east, south or west to the cell underneath =0, and  $\neq$  border
    then
      selected cell move to the empty cell underneath
    end if
    if cell < max_fines then
      transfer fines from north, east, south, or west cells:
      fines_transferred = min(fines in north, east, south or west cell )
      cell += fines_transferred
    end if
    if cell> max_fines then
      transfer fines from north, east, south, or west cells:
      fines_transferred = cell -max_fines
      cell = max_fines
    else
      no fines transfer
    end if
  end for
  count+=1
end while

```

Algorithm 4 Pseudo code/Algorithm for 3D silo discharge model

```

max_fines =maximum fines in a cell (Cell number =10)
min_fines =minimum fines in a cell (Cell number =1)
border= (any number > max_fines)

count=0
while count<discharge cycles, do
  for each cells in height, width, and depth, do
    if any cell = 0 and cell above it ≠ 0, then
      cell moves to the empty cell
    end if
    if cell = 0 and the cell above = 0 and cell north, east, south or west ≠ 0 and cell ≠ border then
      selected cell move to the empty cell underneath
    end if
    if cell < max_fines then
      transfer fines from north, east, south, or west cells:
      fines_transferred = min(fines in north, east, south or west cell)
      cell += fines_transferred
    end if
    if cell > max_fines then
      transfer fines from north, east, south, or west cells:
      fines_transferred = cell -max_fines
      cell = max_fines
    else
      no fines transfer
    end if
  end for
  count+=1
end while

```

Table 10: Calibration data for the Silo 2 filling

	Silo 2 filling	Model predicted outcomes
Maximum fines	10.4	10
Minimum fines	4.6	
Coarse pellets		1
Empty cell		0

Table 11: Calibration data for the Silo 3 filling

	Silo 3 filling	Model predicted outcomes
Maximum fines	12.8	10
Minimum fines	2.3	
Coarse pellets		1
Clean cell		0

Modelling Segregation Phenomena in Large Industrial Silos: A Cellular Automaton Approach

Susantha Dissanayake^a, Hamid Salehi^a, Stefan Zigan^a, Tong Deng^b, Michael Bradley^b

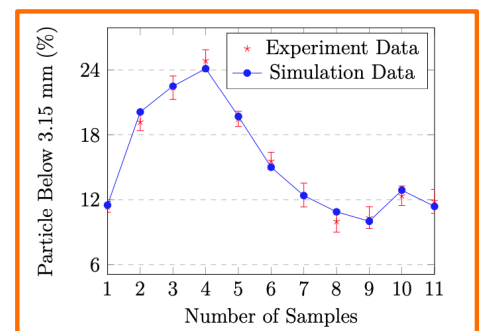
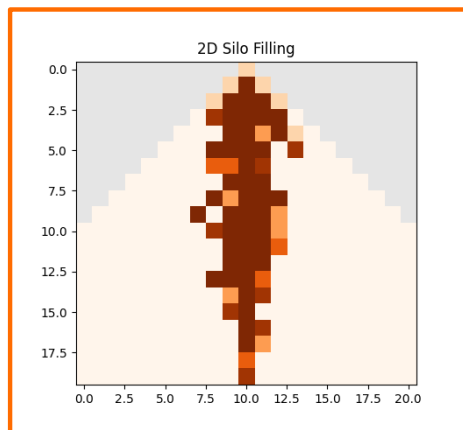
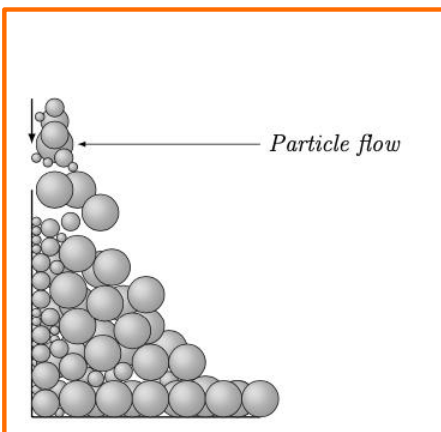
^a*School of Engineering, Faculty of Engineering & Science, University of Greenwich, Central Avenue, Chatham Maritime, ME4 4TB, United Kingdom*

^b*The Wolfson Centre for Bulk Solid Handling Technology, University of Greenwich, Central Avenue, Chatham Maritime, ME4 4TB, United Kingdom*

Email address: s.dissanayake@greenwich.ac.uk (Susantha Dissanayake)

Modelling Segregation Phenomena in Large Industrial Silos: A Cellular Automaton Approach

Method to model segregation in bulk material handling



Journal of Power Technology

Susantha Dissanayake, Hamid Salehi,
Stefan Zigan, Tong Deng, Michael
Bradley

CA modelling

Declaration of interests

The authors declare that they have no known competing financial interests or personal relationships that could have appeared to influence the work reported in this paper.

The authors declare the following financial interests/personal relationships which may be considered as potential competing interests:

Susantha Dissanayake reports financial support was provided by Net Zero research. If there are other authors, they declare that they have no known competing financial interests or personal relationships that could have appeared to influence the work reported in this paper.
